Composites Science and Technology 168 (2018) 104–110

Contents lists available at ScienceDirect

Composites Science and Technology

journal homepage: www.elsevier.com/locate/compscitech

Modelling process induced deformations in 0/90 non-crimp fabrics at the meso-scale

Adam J. Thompson*, Bassam El Said, Jonathan P-H. Belnoue, Stephen R. Hallett

Bristol Composites Institute, Advanced Composites Collaboration for Innovation and Science (ACCIS), University of Bristol, University Walk, Bristol, BS8 1TR, UK

A B S T R A C T

The manufacture of non-crimp fabric composites typically requires the forming and consolidation of the reinforcement material. During this process the material is subjected to complex loading where the coupling of tensile, bending, shear and compressive forces result in deformations to the internal architecture of the textile. To determine the extent of these deformations a numerical modelling method has been developed to capture the kinematic behaviour of non-crimp fabric textiles. This method focuses on capturing the interactions between the fibrous tows and the stitch yarns which bind the tows together. Through modelling at a level of detail in which the meso-scale interactions are explicitly present, the macro-scale behaviour of the material proceeds naturally within the model, negating any requirement for detailed characterisation of the physical material. This also enables a detailed description of the internal architecture of the deformed fabric to be extracted for analysis or further modelling. The present study explores the method's ability to capture both local and global deformations which occur in non-crimp fabrics, specifically to capture the onset of deformations that appear due to tow-stitch interactions and the forming and compaction of multiple layers. Comparison with experimental results show good agreement for both meso-scale deformations, resulting from multi-layer compaction, and global in-plane shear deformations induced through forming over complex tooling.

1. Introduction

The recent growth of fibre reinforced composites for high performance applications has motivated a concentrated effort to increase their performance and sustainability while, simultaneously, reduce their production times and cost. One method of composite production which has the potential to address some of these challenges is Liquid Composite Moulding (LCM). LCM processes are widely used in automotive to cope with high production rates and cost constraints, and are now being exploited in some commercial aircraft programs as the principal material for primary structural components. These processes, unlike pre-pregs and in-autoclave processes, use dry textile preforms which are then infused with a liquid resin. The possibility of eliminating the autoclave process results in significant cost reductions, while the increased thickness and handle-ability of the textiles reduces layup times.

For high performance applications, LCM processes typically use non-crimp fabrics (NCFs). Unlike woven fabrics, where the weaving of orthogonal tows causes the fibres to undulate, tows in NCFs are regarded as having ideal unidirectional fibre paths; where the warp and weft tows are bound together with a light stitch yarn. The stitch yarn ensures the integrity of the fibres is maintained, however, its presence creates distortions to the fibrous tows and can induce deformation mechanisms, during forming processes, which are unique to NCFs.

Distortions to the fibrous structure are introduced to the NCF during its fabrication. These are a result of the penetration of the needle into the fibrous plies during the stitching process. The distortions can be localised to the stitch site, or more global, where the localised distortions collate into large distortions - separating the fibrous tows [1].

The NCF is further susceptible to structural changes during the processing required to achieve the final composite. This typically includes the forming of the initially planar material into a three dimensional shape. During this process the material is subjected to complex loading where the low internal cohesion between tows and fibres allows for large relative displacements to occur. The presence of the stitch yarn constrains these displacements, and hence the deformation mechanisms of the fabric are strongly determined by stitch-tow interactions with stitch strain, stitch architecture and inter-stitch friction all playing an integral role [2–4].

The deformations, which result from the complexity of the stitch yarn and it's interaction with the fibrous tows, have shown to reduce the stiffness and damage resistant capabilities of NCF composites, with tow waviness, resin pockets and tow cross-sectional shape all identified as being key parameters [5–9].

Attempts to model the behaviour of NCFs have focused mainly at the macro-scale, which consider the NCF as a continuum [10], or use semi-discrete methods to include specifics of the meso-scale structure [11]. These methods have been successful at capturing the dominant

* Corresponding author.
E-mail address: adam.thompson@bristol.ac.uk (A.J. Thompson).

https://doi.org/10.1016/j.compscitech.2018.08.029
Received 22 January 2018; Received in revised form 17 August 2018; Accepted 20 August 2018
Available online 31 August 2018

deformations observed during the forming of NCFs, but they are unable to provide details of the deformed meso-scale architecture and have yet to include the high through thickness compliance of the material and interaction of multiple layers.

Discrete methods are an attractive solution for modelling textile materials as they explicitly model the interaction between the individual tows, therefore if sufficient detail of the meso-scale geometry is present within the model then the macro-scale behaviour will appear naturally. Creech et al. [12] compared a discrete modelling approach for the forming of a NCF over a hemisphere with an equivalent continuum approach, the discrete modelling approach proved to be significantly more accurate. This approach used chains of solid elements to represent each individual tow, interconnecting bar elements, approximating the stitch yarn, bound the rows of elements chains together. The authors concluded that the increased accuracy at capturing the macro-scale behaviour of the fabric by the discrete modelling approach was due to the method's ability to capture the relative motions of the individual tows more accurately. However, simplification of the meso-scale structure, namely the tow cross sectional shape and stitch architecture was noted to be a limitation of the method.

A similar approach was developed in Ref. [13] for a ± 45 NCF, this had the addition of gap elements which were placed between tows and allowed for the formed geometry to be used in an infusion model, representing resin flow between fibre tows.

A number of discrete modelling approaches have been proposed for modelling the deformation behaviour of woven textiles. The multi-filament group of methods, which considers yarns to be an assembly of 1D element chains, has proven to be very effective [14–19]. The main benefit of these approaches is their ability to capture the low cohesion and complex interactions between individual fibres and yarns by modelling at the sub yarn level. Nevertheless, the computational cost of modelling at this level is high, this typically constrains the method to modelling at the scale of the unit cell. Stig and Hallström [20] presented a method where the yarns are represented as slender tubes using shell elements. To achieve the initial fabric architecture the tubes are inflated until the required volume is achieved. By capturing the contact between adjacent yarns, during the inflation process, the undulations of the yarns and cross-section shapes were captured to a good degree of accuracy. El Said et al. [21] presented a similar approach for modelling the forming and consolidation of 3d woven fabrics. Implemented in the LS-Dyna Explicit finite element software, the method used a two-step process. The first step generated an accurate as-woven geometry of a unit cell of fabric using a multi-filament approach. The geometry was then extracted and tessellated to form a feature or component scale fabric model, where the yarns are represented as hollow surfaces using shell elements. These elements acted as contact surfaces for yarn to yarn interactions, shell elements were then placed through the thickness to create resistance to transverse compression. This approach proved very successful at generating an accurate as-woven textile architecture and was able to capture both the meso and macro-scale deformations of the fabric induced by its forming and consolidation.

The present paper extends the method proposed by El Said et al. [21] to capture the complex interactions between the stitch yarn and the fibrous tows in a biaxial NCF during forming and compaction processes. The challenge of generating an accurate initial geometry is first addressed through the use of a multi-chain beam element approach at the unit cell scale. This geometry is then tessellated to build a macro-scale fabric model which is used to examine the forming and consolidation behaviour of both single and multiple layers of NCFs.

2. Modelling initial geometry

The fabrication of NCFs results in distortions to the individual tows within the fabric. Specifically, the penetration of the needle into the unidirectional plies, and tension applied to the stitch yarn, can cause inter-tow separation and undulation along the length of the tows [1]. Representing the manufactured fabric architecture accurately in the modelling process has been shown to increase the accuracy of the models for predicting the deformation of the meso-scale structure [22]. The first stage of this modelling process will therefore focus on the acquisition of an accurate initial geometry, this will then be used for the subsequent modelling of forming and consolidation processes.

2.1. Modelling strategy

The multi-filament group of methods has shown notable accuracy in predicting the as-woven and compacted state of 2D and 3D woven fabrics [14–19]. A number of methods exist within in this modelling category, however they all share the same premise. They discretise each tow into multiple 1D element chains, each of these element chains approximates the behaviour of a bundle of fibres. Contact models are then used to capture the interactions between the element chains, this allows for both the low cohesion and complex interactions of the fibres to be simulated.

The approach used here, to model the as-manufactured state of the NCF, will be based on a multi-filament method initially proposed by Mahadik and Hallett [16] for 3-D woven fabrics. This approach uses chains of beam elements to represent the bundles of fibres, these are assigned an elastic, perfectly plastic material behaviour which is used to approximate the bending behaviour of bundles of fibres. The model begins with an initially loose description of the fabric architecture, which is built based on the kinematics of the weaving process. An artificial thermal expansion coefficient is prescribed to the beam elements representing the binder yarns. By applying a negative thermal load to the model, the beam elements in the binder yarn contract, which simulates the tension on the tow, during the weaving process and generates the initial as-woven fabric geometry.

For NCFs, the fibrous tows are not inter-woven, however the stitch yarn assumes the same purpose during the stitching process as the binder yarn does during the weaving process of 3-D woven fabrics - it binds the warp and the weft tows together. Based on this, the same modelling methodology is applicable to simulate the stitching process of NCFs.

2.2. Prediction of initial geometry

The fabric under consideration in this paper is a carbon fibre, two layer, biaxial NCF. The warp and the weft tows are arranged in a 0/90 configuration. The areal weight of each of the warp and weft layers is 268 gm^{-2}. These are bound together with a light polyester stitch yarn in a tricot chain formation which has an areal weight of 4 gm^{-2}, the total areal weight of the material equating to 540 gm^{-2}. The stitching process is periodic, therefore the structure is built up of repeating cells. This periodicity can be exploited in the modelling of the stitch process by using just a single unit cell to simulate the behaviour of the entire structure. The chosen unit cell must capture the overall periodicities of the fabric so that, through translations and repetitions, the entire fabric can be constructed. Fig. 1 illustrates the unit cell that will be used in this modelling process. The unit cell dimensions are 10 mm along the warp direction and 5 mm along the weft. It should be noted that complex interactions of the stitch yarn, specifically at the loop regions of the chain stitch, are not present at the boundaries of the unit. This simplifies the periodic boundary constraints, which are required in the model to ensure the periodicity of the structure is maintained.

The approximate number of fibres contained within each stitch repeat in the unit cell was calculated under the assumption that each stitch loop in the respective direction contains equal number of fibres, fibres do not bridge between tows and the fibre paths are perfectly straight across the unit cell. Using the areal weight of each layer, the unit cell dimensions, fibre density (1,770 kgm^{-3}) and fibre diameter (7 μm) the approximate number of fibres in the warp tows is 20,000 and in the weft tows 10,000.

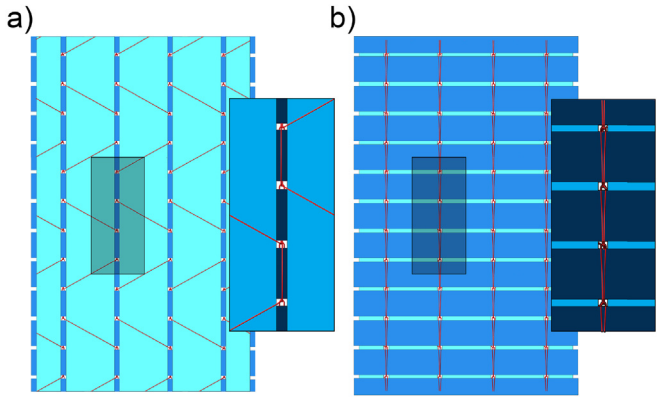

Fig. 1. a) top view of fabric highlighting a single unit cell b) bottom view of fabric highlighting a single unit cell.

Table 1
Material properties applied to beam elements.

ρ (tonne/mm^2)	E (MPa)	σ_y (MPa)
0.05	20	40

Following the approach proposed by Mahadik and Hallett [16], each of the fibrous tows in the model is constructed of beam element chains and assigned with a plastic kinematic material model available in the LS-Dyna explicit finite element software package. Based on [23] the base number of beam element chains per tow is set to 64, each beam element representing approximately 155 fibres. Conserving this beam-to-fibre ratio results in 64 chains in the weft tows and 128 in the warp tows. Each beam element chain has a circular cross section, the area of which is determined by the sum of the cross section areas of the fibres each element chain represents. The stitch yarn is simplified to just a single beam element chain. Green et al. [23] made further developments to the model proposed in Ref. [16], the properties for the plastic kinematic material model were tailored to increase the accuracy of the model, these parameters are shown in Table 1 and will be used here for the NCF model.

The geometry of the initial state of the model is illustrated in Fig. 2. An initially loose topology of the fabric architecture is generated. This is based on the kinematics of the stitching process and is constructed from basic information of the fabric i.e. stitch architecture, tow spacing, the number of fibres per tow and diameter of each of the fibres.

As just a single unit cell is used, it is necessary to consider the effect of adjacent cells to enforce the periodicity in the model. For the beam element chains representing the fibrous tows, multi-point constraints (MPCs), which set restrictions on the mutual displacement of linked nodes, connect tow end nodes to the equivalent node on the opposite side of the unit cell. This constrains the tows in the length direction, however, as half tows are present at the boundaries of the unit cell, further constraints are required to stop transverse spreading of the tow outside the unit cell, which would compromise the periodicity of the model. To enforce this constraint, the model is expanded to include a small area of the adjacent unit cells. This is done by taking the tows present at the boundaries of the unit cell, copying and translating them laterally to the opposite side of the unit cell. The copied yarns act as slave yarns and sit outside the unit cell boundary, each node within the slave yarn is linked to its duplicate within the unit cell in all degrees of freedom through the use of MPCs. A schematic showing the initial model, including the slave tows, is shown in Fig. 2.

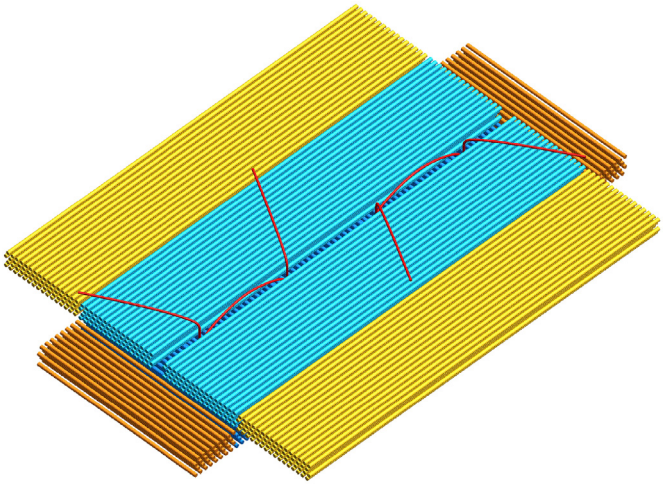

Fig. 2. Full model of NCF in its initial loose state.

To achieve the initial fabric architecture, a thermal expansion coefficient is prescribed to the beam elements that represent the stitch yarn. The model is then subjected to a negative thermal load, which contracts the individual beam elements. As periodic boundary conditions constrain the nodes at the boundaries, the contraction of the individual beam elements results in tension of the beam element chain, simulating the tension applied to the stitch yarn during the stitching process. This draws the fabric together and generates the initial architecture. The thermal load is used as a method to apply an even strain to the stitch yarn to reduce its length. The magnitude of this load is such that the final length of the stitch chain matches that in the physical material. This can be approximated using the areal weight of the stitch yarn in the fabric and its tex value; parameters which are often readily available from the material provider. Fig. 3 illustrates the process and also emphasises the role of the slave tows.

3. Meso-macro model

The multi-chain beam element method discussed in the previous section is used to generate the initial state of the NCF geometry. It is a high resolution method which is able to approximate the low cohesion and complex interactions of the individual fibres within a single tow. The discretisation of the tows into multiple element chains, however, confines the method to unit cell size problems and it is therefore not computationally feasible to model the non periodic deformations that are typically present in the forming and consolidation of complex structures. A method is developed here which allows for larger scale models, comprised of hundreds of unit cells, to be built and used for simulating non periodic problems. This utilises the predicted NCF geometry from the previous section to build a more computationally efficient model able to capture the meso-scale deformations, as well as the macro-scale behaviour, of the fabric.

3.1. Geometry extraction and tessellation

To have a macro-scale model that is able to simulate both the meso and macro-scale deformations of the textile structure, an accurate representation of the meso-scale structure is first required. This was achieved in the previous section, but for this to be exploited in a larger scale model, the geometric features must be extracted so that the fibrous structure of each of the tows can be represented as a single surface. Two steps are required to perform this. First the centreline of each tow is extracted and defined by a series of centreline points. Next, a set of section points forming the tow cross-section surface, at each centreline point, is defined in a local coordinate system perpendicular to the centreline.

Following the extraction of the tow surface geometry a finite element model needs to be constructed. The is done by tracing the surface of the individual tows with shell elements, these shells act as contact surfaces which allow for tow interactions to be captured. However,

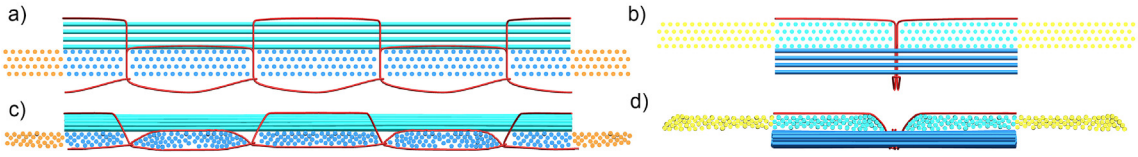

Fig. 3. Initial loose geometry a) weft cross-section b) warp cross-section. Predicted as-manufactured geometry c) weft cross-section d) warp cross-section.

Table 2
Tow surface shell element material properties for elasto-plastic material model.

Shear Modulus (MPa)	Tangential Modulus (MPa)	Bulk Modulus (MPa)	Yield Strength
5	100	200	60

Table 3
Tow core shell element material properties for visco-elastic material model.

Initial Shear Modulus (MPa)	Infinite Shear Modulus (MPa)	Bulk Modulus (MPa)	Decay Constant
25	50	200	0.1

modelling just the surface geometry with shell elements results in tows with hollow sections, which have no resistance to transverse loading. To simulate the transverse behaviour of the tow accurately, shell element supports are place along the length of the tows. These are prescribed with a visco-elastic material property to enable cross-section deformation to be simulated as a shear dominated phenomenon. The properties for the shell elements representing the tow surface and the shell element supports are presented in Tables 2 and 3 respectively. These have been pragmatically tailored to capture the deformation behaviour of carbon fibre tows and are discussed in detail in Ref. [21]. It should be noted that these are effective properties and hence do not preserve the physical properties of the real tow structure, therefore the method considers only the kinematic behaviour of the fabric structure and not its mechanical response.

The nodes of the deformed beam element chain, representing the stitch yarn, are imported from the multi-filament model. The number of nodes, representing the stitch yarns, are reduced and redistributed ensuring the geometry is accurately maintained. The stitch yarns are then re-meshed and represented again as a single beam element chain, prescribed with the same plastic kinematic material model properties defined in section 2.2. A schematic of the new representation of the fabric geometry can be seen in Fig. 4.

Following the geometry extraction and the re-meshing of the unit cell model, it is then tessellated to a specified size, which is dependent on the process is to be modelled. This builds a fabric model of multiple unit cells that can be used to examine larger scale processes.

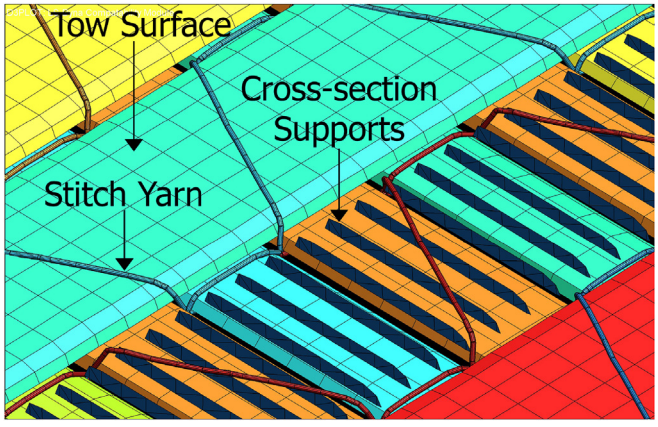

Fig. 4. Mesh for 3D tow representation with one tow hidden to show cross-section supports.

3.2. Compaction of multiple layers

The compaction of dry fibre reinforcements is an integral process in composite manufacture, to increase the fibre volume fraction in the final composite. To validate the compressive behaviour of the meso-macro model, the compaction of five layers of the biaxial NCF was performed and compared to μCT images. To obtain the μCT images five layers of the biaxial NCF were compacted, in their dry state, using the bespoke acrylic compaction rig. Analysis of the compressed fabric in its dry state eliminated the possible deformations which could form as a result of the infusion process, ensuring the deformations present were solely a product of the compaction process. The layers were stacked up all with the same fibre orientation, the relative shift between layers was not controlled. Spacers were used in the compaction rig to control the final thickness of the specimen, which was equivalent to 60% fibre Vf.

For the model, the unit cell geometry was extracted and tessellated, to the same size as the physical specimen, following the procedure previously outlined. The relative shifts, present between layers in the experiment, were extracted from the μCT images and applied to the model. The model was then compacted between two parallel rigid surfaces via a velocity controlled displacement to a fibre volume fraction of 60%.

A comparison between the compacted geometries of the μCT observations and the simulation are presented in Fig. 5. The prediction for the tow cross sectional shapes show good agreement with experimental results. Furthermore the model is able to predict the tow paths with good accuracy, capturing the small undulations in the tow that form as a result of the tows having to accommodate the crossing stitch yarn.

3.3. Forming over complex tooling

When a planar material is draped or formed over complex three dimensional tools, the material is forced to deform to allow for a change in its shape. For textiles, in-plane shear is the dominant deformation mechanism during this process, this results in large rotations in the fibre direction and a change in the net shape of the material. The extent of the shear deformation is largely determined by the tool shape. Doubly

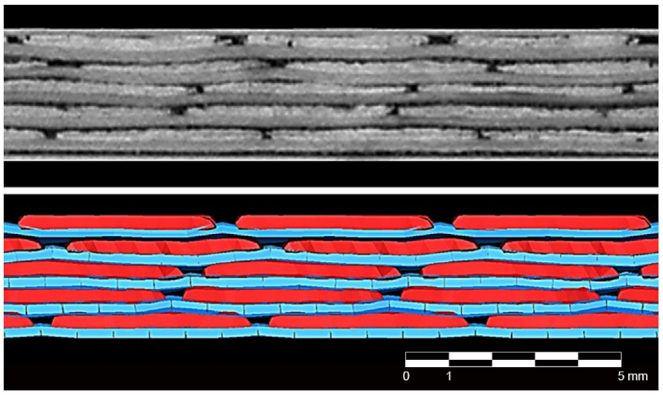

Fig. 5. A comparison between μCT image of compacted NCF layers (top) and model prediction (bottom).

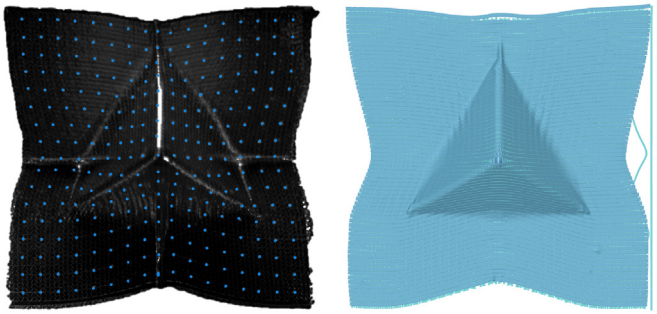

Fig. 6. Single layer of NCF formed over Tetrahedron. Experiment results shown on the left and simulated shown on the right.

curved tools such as tetrahedrons and double domes are often used as bench mark problems for examining the shear behaviour of textiles. To examine the meso-macro method's ability to capture the shear behaviour of the NCF the forming of a single layer over a tetrahedron was simulated and compared with experimental results.

For the experiment, a specimen size of 350 × 350 mm was used. A grid of dots with 20 mm spacing was placed on the top surface of the fabric. This was then formed over a tetrahedron tool using a double diaphragm forming process. An image was taken from above the fabric, normal to the diaphragm surface, before and after forming, to track the dotted grid between the two steps.

The double diaphragm forming process is a controlled method which creates an even tension across the fabric whilst not inhibiting out of plane deformation. The process consists of three steps. In the first step, the fabric is placed between two elastomeric diaphragms. The diaphragms are positioned and secured over a hollow vacuum forming box with the forming tool beneath the fabric on a liftable surface. Full vacuum is then applied to the cavity between the diaphragms. The second step is to raise the surface with the tool on so that it is aligned to the external boundaries of the membranes. The final step is then to evacuate the air between the bag and the tool surface. The atmospheric air pressure pushes the diaphragms down, forcing the fabric to form to the tool geometry.

In order to model the experiment the simulated forming process was simplified. Again the unit cell geometry was extracted and tessellated to a size of 350 × 350 mm. A rigid surface was placed just below the bottom surface of the fabric. A body load was then applied to the modelled fabric, compressing the NCF against the rigid plate. The tetrahedron tool was then translated upwards, the contact between the tetrahedron and the rigid plate was removed enabling the tetrahedron to penetrate through the plate and allow the NCF to be formed over it. Fig. 6 shows a comparison between the experiment and predicted formed configurations.

The images of the NCF in its un-deformed state and final configuration have been digitally processed to extract the coordinates of the grid points. The detection process starts by enhancing the images of the physical grid by overlaying circles on the grid points. Next the images are submitted to an extraction algorithm that detects the circles and extracts the centre points. A mesh is then built using the grid points. This mesh can be used to calculate the shear angle throughout the preform. It should be noted that this is only the deformation from the top-view and is not actual in-plane shear angles as the deformation cannot be resolved to the fabric surface normal from the top views images alone. Nonetheless, this is still a useful comparative measure between the experiment and the finite element analysis when both results are processed in the same way. To ensure the results were directly comparable, the dotted grid taken from the experiment prior to forming was extracted and projected on the surface of the modelled fabric. The nearest node to each of these points was then tracked through the simulated forming process and extracted when the simulation was complete.

An overlay of the two deformed meshes from the experiment and the simulation is shown in Fig. 7a. This comparison shows that the simulation is in good agreement with the experimental work for predicting the global fabric deformation. Localised differences are present, particularly around the base of the punch tool. The top view shear angles calculated from these grids (shown in Fig. 7b) present a similar result. The simulation follows the general trend from the experiment but there are local differences present in the experiment which are not realised in the simulation. This may be attributed to the simplification of the boundary conditions in the simulation not being fully

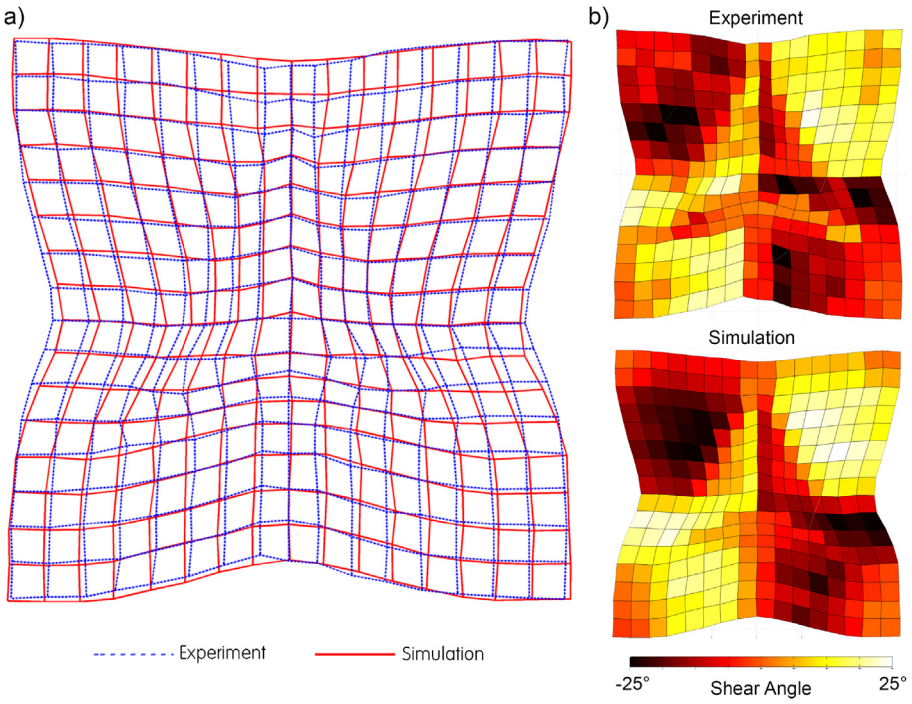

Fig. 7. A comparison between the experimental and simulated post-formed fabric geometries a) overlay of extracted grids b) Gradient plots of planar shear angles.

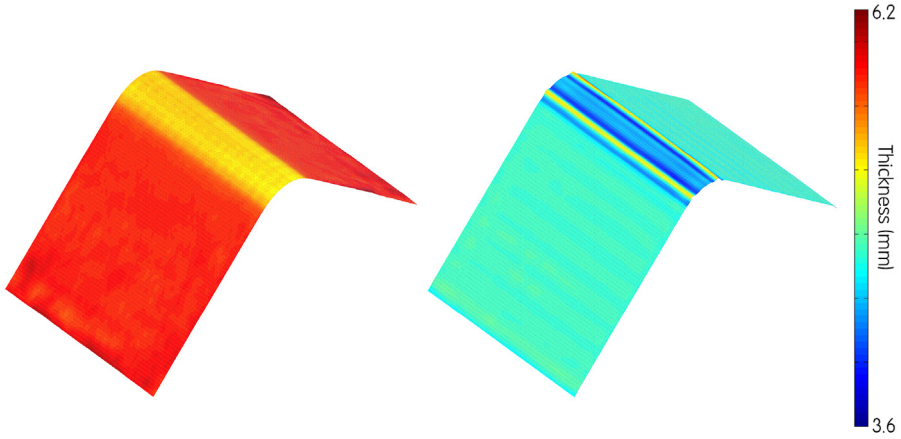

Fig. 8. Surface gradient plot showing the thickness variation of the layup before compaction (left) and after compaction (right).

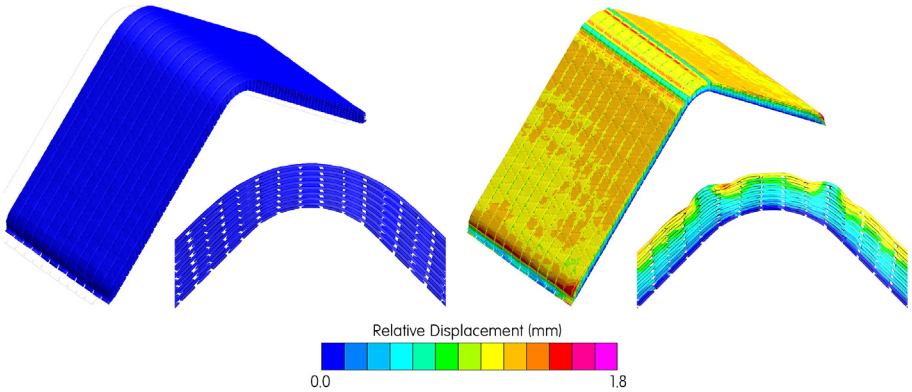

Fig. 9. Gradient plots showing the relative displacement from initial formed geometry (top) to compacted geometry (bottom).

representative of the double diaphragm forming process used in the experiment.

3.4. Forming and compaction of multiple layers

Fibrous materials are highly compliant in the plane transverse to the fibre direction - with the application of low pressures their thickness can be significantly reduced. When coupled with even simple geometries, this high compliance can result in the formation of wrinkles. A typical example of this is the compaction of multiple layers over a simple male radius. When compacted, the external radius of the lay-up is reduced, producing an excess length of material. If the material is constrained in-plane, via inter ply friction or other geometric features, the excess material in the radius is unable to migrate and hence is forced to deform out of plane to accommodate it, resulting in the formation of wrinkles.

To determine whether the shell based forming approach is capable of simulating the mechanisms behind these deformations, the forming and compaction of eight layers of the NCF over a simple L-section tool is simulated. The forming phase was performed by placing the layers of NCF on top of a rigid surface. A body load was then applied to each layer, forcing adjacent layers to come into contact and the lay-up to be in contact with the rigid plate. A rigid surface representing the L-section tool is then translated upwards using a velocity controlled displacement. The contact between the L-section and the rigid plate is neglected, allowing for the tool to penetrate through the rigid surface and for the layers of NCF to be formed over the L-section.

Following the forming phase, a surface representing a vacuum bag is then placed into the model, this is modelled using shell elements with isotropic material properties. The displacement degrees of freedom at the ends of the bag are given a fixed condition, and a ramped pressure is applied to the surface of the bag. This pressure compresses the NCF layers against the L-Section tool, the simulation was stopped when a thickness equivalent to 60%Vf was achieved at the centre of the radius.

Fig. 8 shows the thickness variation of the layup, across the L-section, pre and post compaction. The model prior to compaction has a lower thickness at the radius than in the arms of the L-section. During the forming process the layup is forced to stretch and deform to conform to the radius, this causes a higher pressure to be exerted on the layup at this region, resulting in a reduced thickness. After compaction the centre of the radius still exhibits a lower thickness, however, the compaction has encouraged wrinkles to form at its edges. Fig. 9 highlights the wrinkle formation in more detail, showing the resultant displacement of the model from pre-compaction to post-compaction. It is clear that two large wrinkles have formed at the edges of the radius and a third, with a smaller wave height, but larger wave length, has begun to form in the centre of the radius. This shows a similar trend to what has been observed in Ref. [24].

4. Conclusions

This paper has introduced a meso-scale modelling approach for predicting the forming and compaction of NCFs over simple and more complex geometries. Initial fabric geometry has been predicted using a unit cell multi-filament modelling method. This has been used to capture the interaction of the stitch yarn with the fibrous tows during the stitching process. The predicted geometry has then been used to generate a more computational efficient meso-macro model, which is able to predict both local and global deformations of the NCF during forming and compaction processes.

The method has been compared with experimental results to determine its validity for use in simulating both forming and compaction processes of a non-crimp fabric. The accuracy of the predictions has highlighted its ability to capture the meso-scale deformations, which occur during compaction, i. e undulations of fibre path and changes to tow cross section shape, and the large scale shear deformations induced by the forming of a tetrahedron. Furthermore, the method has been able to simulate the large transverse compliance of the material and inter-ply interactions, both of which encourage the formation of wrinkles during the compaction of multiple layers over simple curved tooling, as shown in section 3.4.

By explicitly modelling the meso-scale structure and the complex interactions that occur at this scale, the method is able to predict the deformations of the material, independent of any experimental characterisation of the physical specimen. The transfer of the properties and methodology used for 3D woven fabrics, presented in Refs. [21] and [23], to model NCFs, highlights the flexibility of the method - showing its ability to model a wide range of fabric architectures. The method would benefit from the inclusion of the real material properties of the physical constituents within the model, but, as a method to examine purely the deformations of the fibrous structure, this kinematic approach has proven to be very capable.

The possible use of high fidelity deformation models, like the one proposed here, ranges from the design and optimisation of new textiles and manufacturing processes, to pre-processors to generate the geometry for mechanical analysis of the final composite part. Although their computation expense is significantly higher than their continuum based counterpart, the continual increase in computational power is encouraging and makes their use increasingly more feasible within a design environment.

Acknowledgements

This work was funded by the EPSRC through the Doctoral Training Partnership (DTO) grant to the University of Bristol (EP/L504919/1) and the Centre for Innovative Manufacturing in Composites EPSRC project ”Defect Generation Mechanisms in Thick and Variable Thickness Composite Parts - Understanding, Predicting and Mitigation” (DefGen), (EP/I033513). All data to support the conclusions reached are included in this article.

References

[1] S.V. Lomov, 4 - understanding and modelling the effect of stitching on the geometry of non-crimp fabrics, Non-crimp Fabric Composites, Woodhead Publishing, 2011, pp. 84–102.
[2] K. Potter, Influence of the detailed structure of two variants of non-crimped carbon fabric on the drape properties, Advanced Composite Letters 11 (6).
[3] H. Kong, A.P. Mouritz, R. Paton, Tensile extension properties and deformation mechanisms of multiaxial non-crimp fabrics, Compos. Struct. 66 (1–4) (2004) 249–259.
[4] S. Bel, P. Boisse, F. Dumont, Analyses of the deformation mechanisms of non-crimp fabric composite reinforcements during preforming, Appl. Compos. Mater. 19 (3–4) (2011) 513–528.
[5] S. Drapier, M.R. Wisnom, A finite-element investigation of the interlaminar shear behaviour of non-crimp-fabric-based composites, Compos. Sci. Technol. 59 (16) (1999) 2351–2362.
[6] S. Drapier, M.R. Wisnom, Finite-element investigation of the compressive strength of non-crimp-fabric-based composites, Compos. Sci. Technol. 59 (8) (1999) 1287–1297.
[7] D. Mattsson, R. Joffe, J. Varna, Methodology for characterization of internal structure parameters governing performance in ncf composites, Compos. Part B Eng. 38 (1) (2007) 44–57.
[8] H. He, N. Himmel, Structurally stitched ncf cfrp laminates. part 1: experimental characterization of in-plane and out-of-plane properties, Compos. Sci. Technol. 71 (5) (2011) 549–568.
[9] L.M. Ferreira, E. Graciani, F. Pars, Modelling the waviness of the fibres in non-crimp fabric composites using 3d finite element models with straight tows, Compos. Struct. 107 (2014) 79–87.
[10] W.-R. Yu, P. Harrison, A. Long, Finite element forming simulation for non-crimp fabrics using a non-orthogonal constitutive equation, Compos. Appl. Sci. Manuf. 36 (8) (2005) 1079–1093.
[11] S. Bel, N. Hamila, P. Boisse, F. Dumont, Finite element model for ncf composite reinforcement preforming: importance of inter-ply sliding, Compos. Appl. Sci. Manuf. 43 (12) (2012) 2269–2277.
[12] G. Creech, A.K. Pickett, Meso-modelling of non-crimp fabric composites for coupled drape and failure analysis, J. Mater. Sci. 41 (20) (2006) 6725–6736.
[13] J. Sirtautas, A.K. Pickett, P. Lpicier, A mesoscopic model for coupled drape-infusion simulation of biaxial non-crimp fabric, Compos. Part B Eng. 47 (2013) 48–57.
[14] G. Zhou, X. Sun, Y. Wang, Multi-chain digital element analysis in textile mechanics, Compos. Sci. Technol. 64 (2) (2004) 239–244.
[15] D. Durville, Simulation of the mechanical behaviour of woven fabrics at the scale of fibers, Int. J. Material Form. 3 (S2) (2010) 1241–1251.
[16] Y. Mahadik, S.R. Hallett, Finite element modelling of tow geometry in 3d woven fabrics, Compos. Appl. Sci. Manuf. 41 (9) (2010) 1192–1200.
[17] O. Dbrich, T. Gereke, C. Cherif, Modelling of textile composite reinforcements on the micro-scale, Autex Res. J. 14 (2014) 28–33.
[18] S. Joglekar, M. Pankow, Modeling of 3d woven composites using the digital element approach for accurate prediction of kinking under compressive loads, Compos. Struct. 160 (15 January 2017) 547–559.
[19] L. Daelemans, J. Faes, S. Allaoui, G. Hivet, M. Dierick, L. Van Hoorebeke, W. Van Paepegem, Finite element simulation of the woven geometry and mechanical behaviour of a 3d woven dry fabric under tensile and shear loading using the digital element method, Compos. Sci. Technol. 137 (2016) 177–187.
[20] F. Stig, S. Hallstrm, Spatial modelling of 3d-woven textiles, Compos. Struct. 94 (5) (2012) 1495–1502.
[21] B. El Said, S. Green, S.R. Hallett, Kinematic modelling of 3d woven fabric deformation for structural scale features, Compos. Appl. Sci. Manuf. 57 (2014) 95–107.
[22] N. Naouar, E. Vidal-Salle, J. Schneider, E. Maire, P. Boisse, Meso-scale fe analyses of textile composite reinforcement deformation based on x-ray computed tomography, Compos. Struct. 116 (2014) 165–176.
[23] S.D. Green, A.C. Long, B.S.F. El Said, S.R. Hallett, Numerical modelling of 3d woven preform deformations, Compos. Struct. 108 (2014) 747–756.
[24] T.J. Dodwell, R. Butler, G.W. Hunt, Out-of-plane ply wrinkling defects during consolidation over an external radius, Compos. Sci. Technol. 105 (2014) 151–159.